Electronic Supplementary Information

One-Step Facile Synthesis of *fcc* Ru-RuO_2 Activates Superior Bifunctionality toward Overall Alkaline Water Splitting

Qianqian Fan[a], Yueyue Shao[b], Longzhou Zhang[c], Jia Zhou*[b], Guigen Wang *[a]*

[a]Guangdong Provincial Key Laboratory of Semiconductor Optoelectronic Materials and Intelligent Photonic Systems, School of Materials Science and Engineering, Harbin Institute of Technology, Shenzhen, Shenzhen 518055, China

[b]State Key Laboratory of Urban Water Resource and Environment, School of Science, Harbin Institute of Technology, Shenzhen 518055, China

[c]Electron Microscope Center, Yunnan University, Kunming, 650091, China

These authors contributed equally to this work.

These authors contributed equally to this work.

Figures

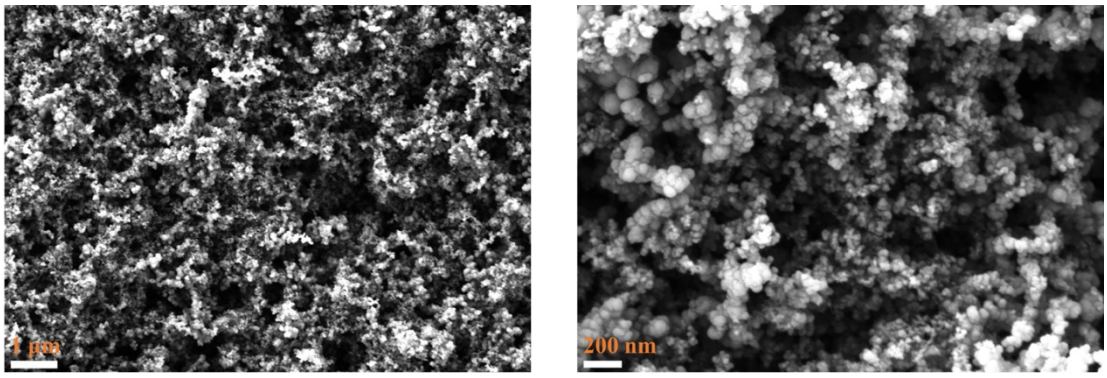

Fig. S1. SEM images of the pristine carbon black at different scales.

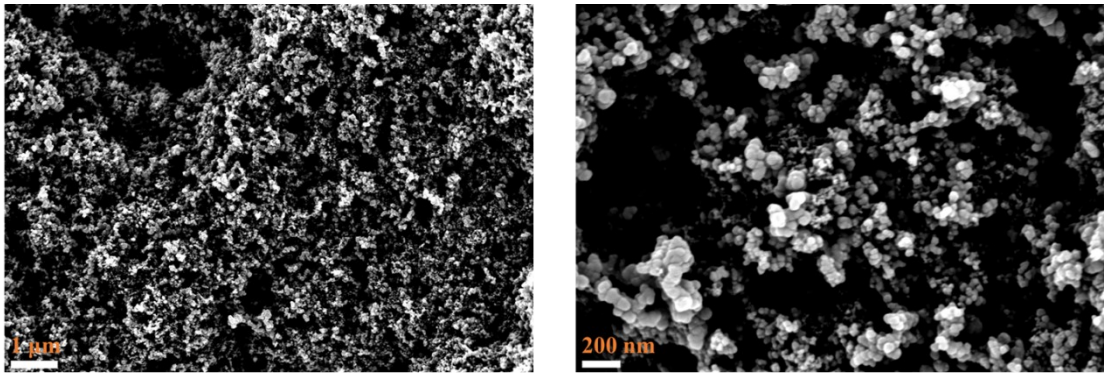

Fig. S2. SEM images of the Ru-RuO_2/C at different scales.

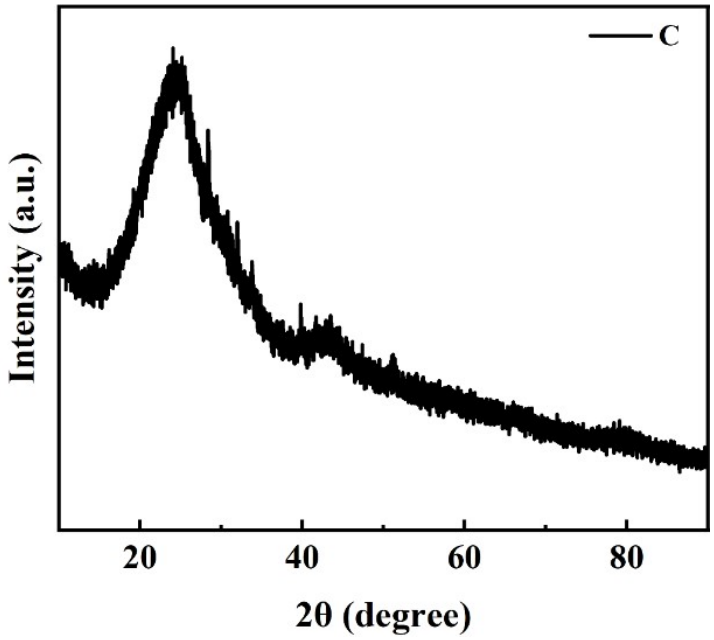

Fig. S3. XRD characterization of the conductive carbon black.

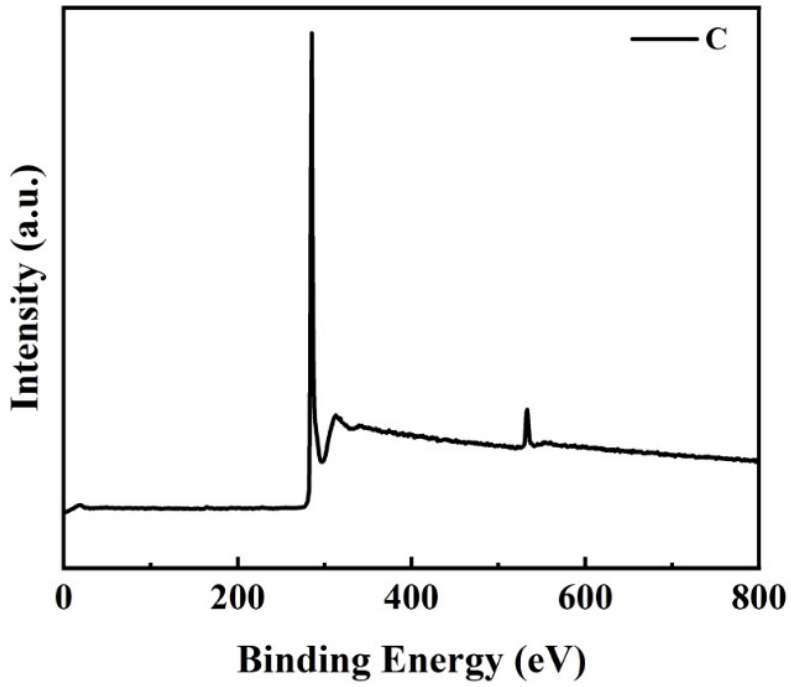

Fig. S4. The survey of High resolution XPS spectra of C

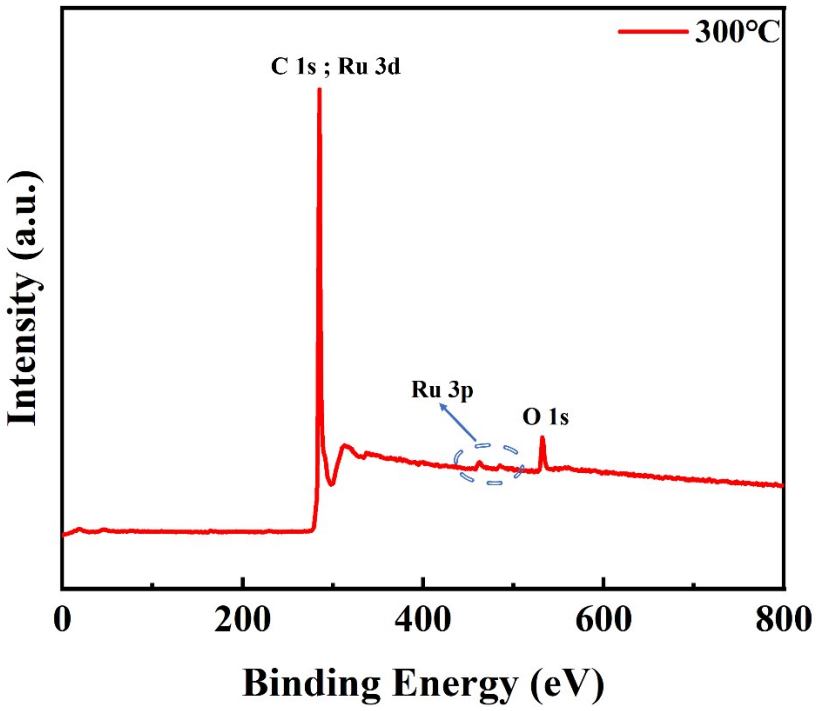

Fig. S5. The survey of High resolution XPS spectra of *fcc* Ru-RuO_2/C.

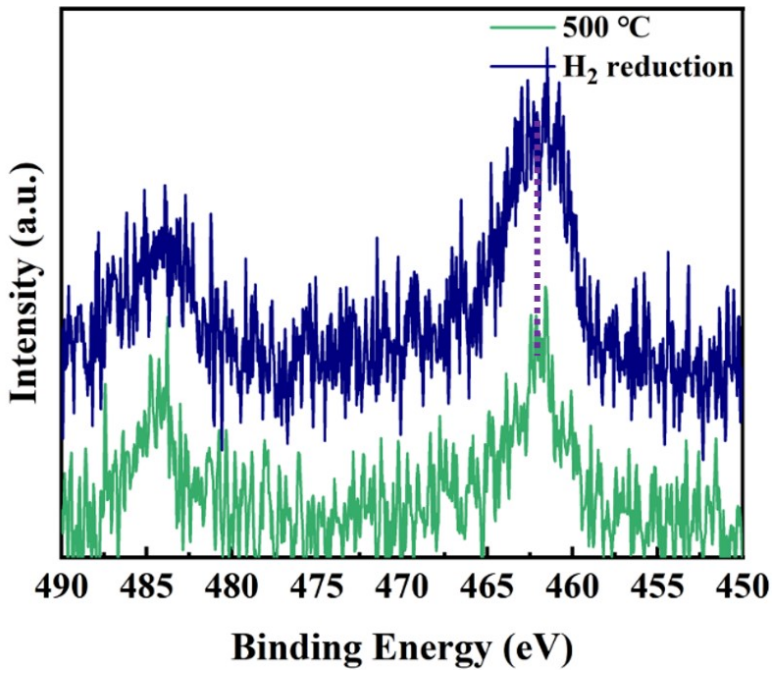

Fig. S6. XPS Ru 3p peaks of the 500℃ and H_2 reduction.

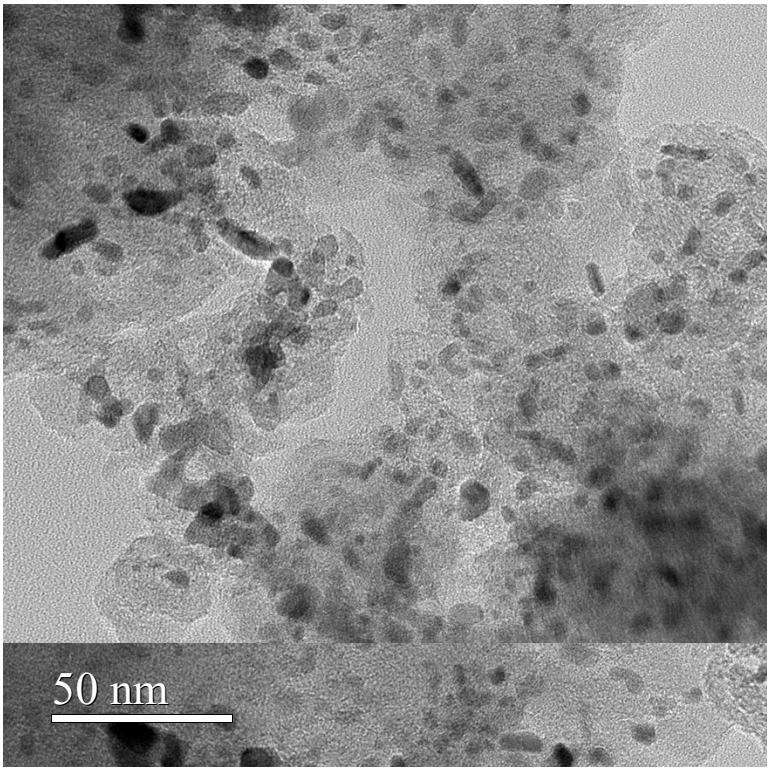

Fig. S7. High-magnification TEM image of the *fcc* Ru-RuO_2/C.

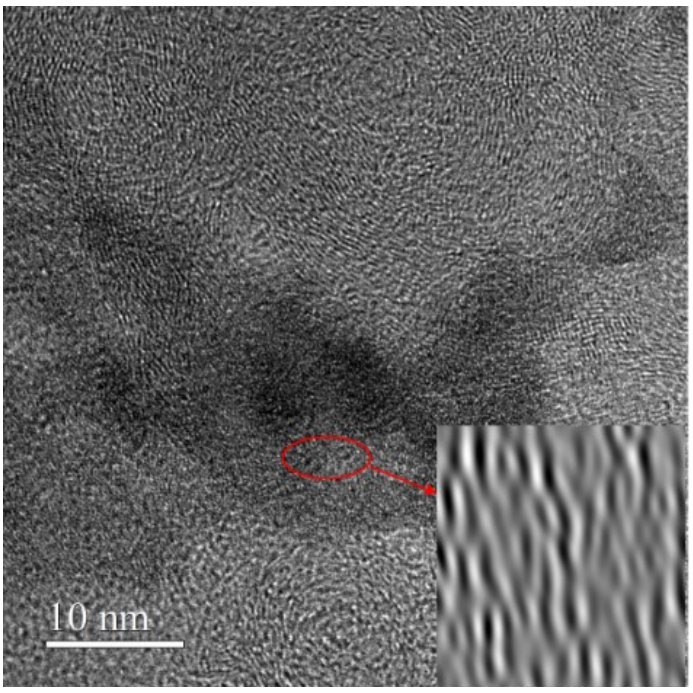

Fig. S8. High-magnification TEM image of the 200 ℃.

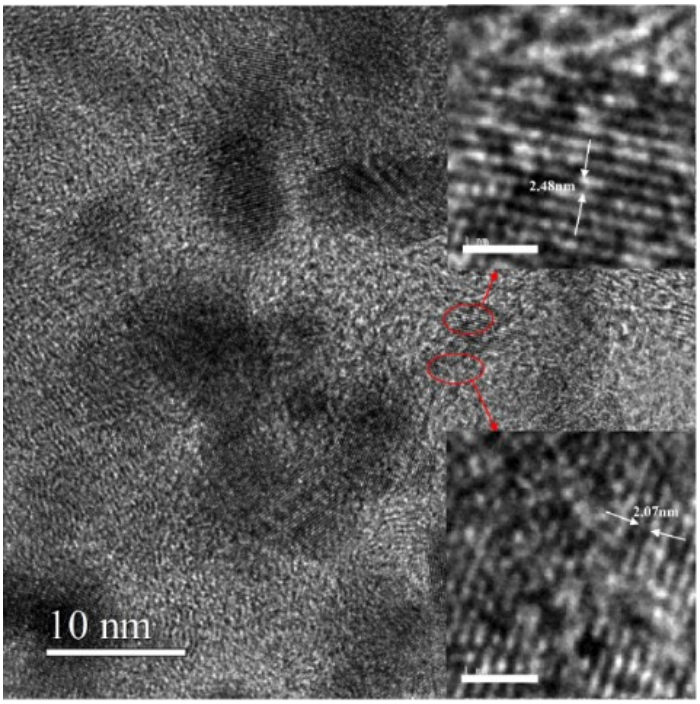

Fig. S9. High-magnification TEM image of the 400 ℃.

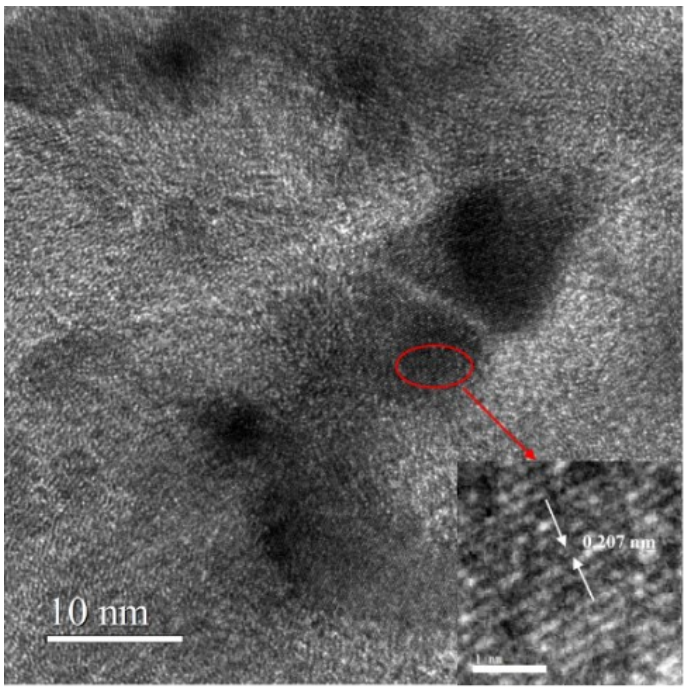

Fig. S10. High-magnification TEM image of the 500 ℃.

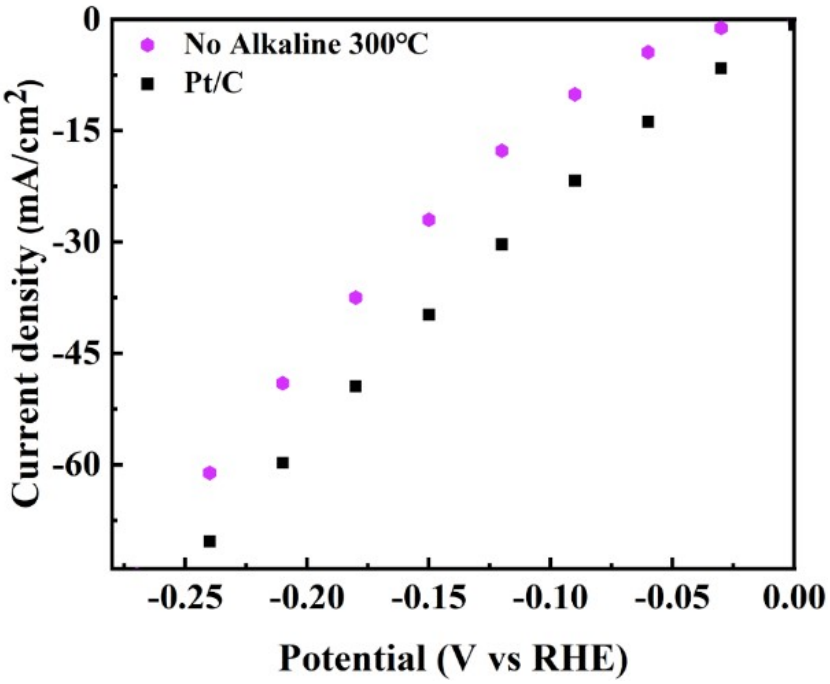

Fig. S11. Comparison of electrocatalytic HER performance of 20 % Pt/C.

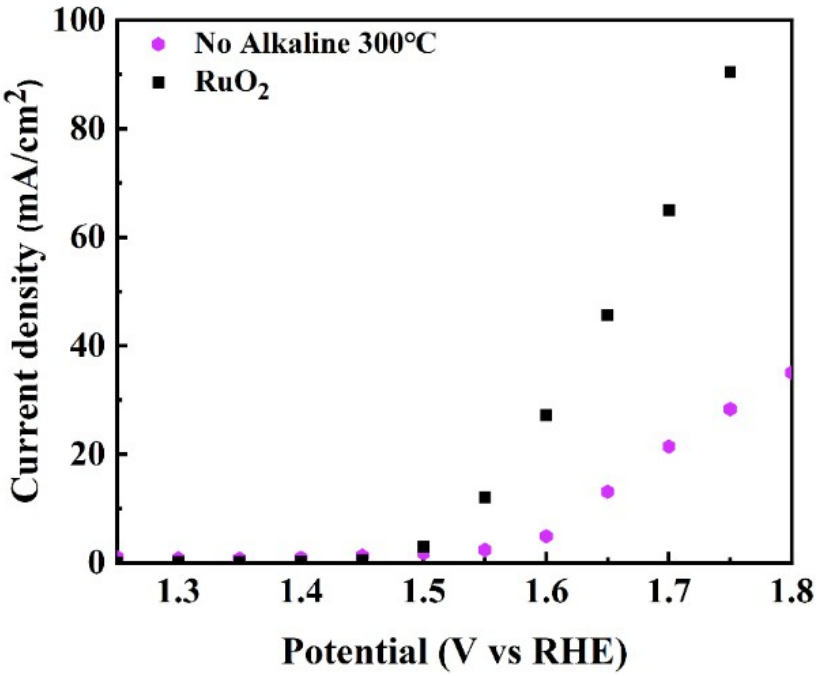

Fig. S12. Comparison of electrocatalytic OER performance of RuO_2.

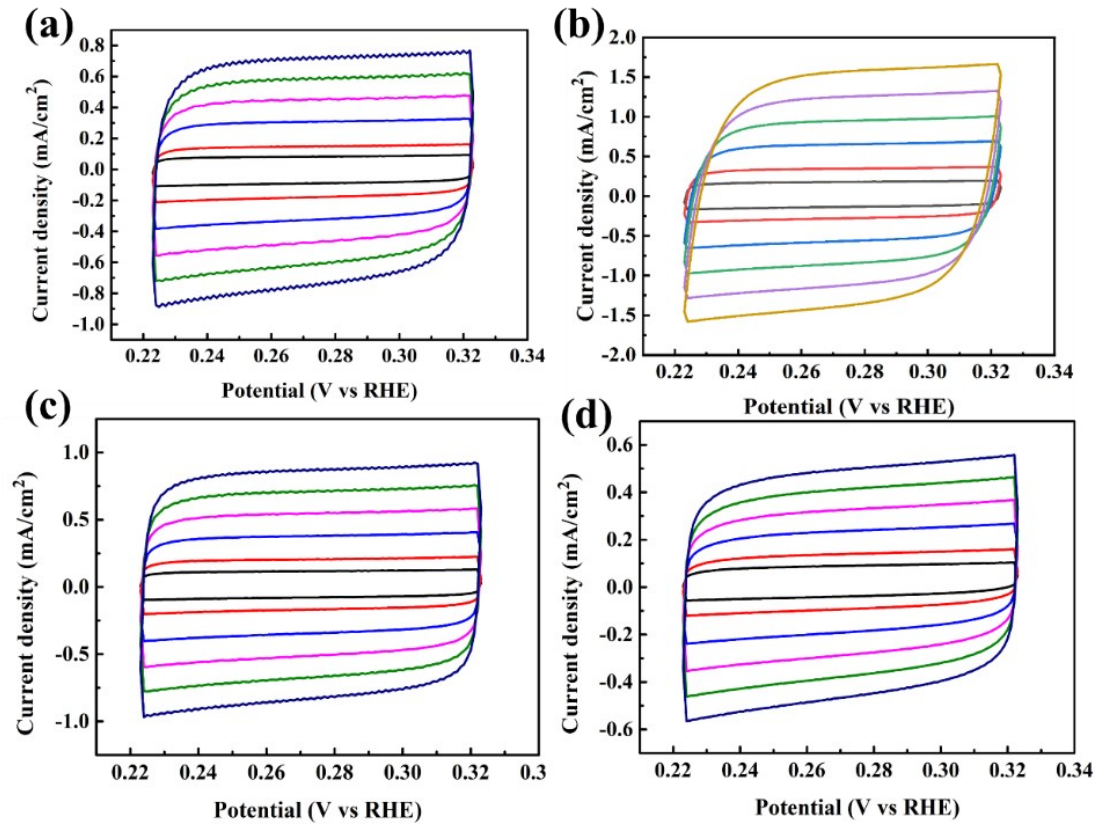

Fig. S13. Cyclic voltammetry curves: (**a**) 200 ℃, (**b**) 300 ℃, (**c**) 400 ℃ and (**d**) 500 ℃, tested under the potential window of 0 V-0.1 V vs. RHE under different scan rates.

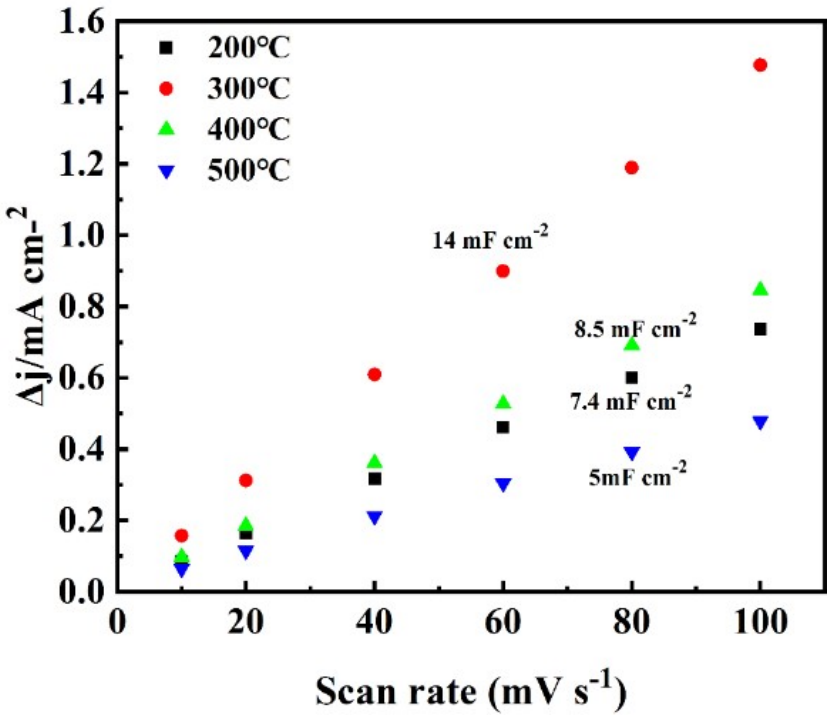

Fig. S14. Electrochemical double-layer capacitances (C_{dl}) at different annealing temperatures.

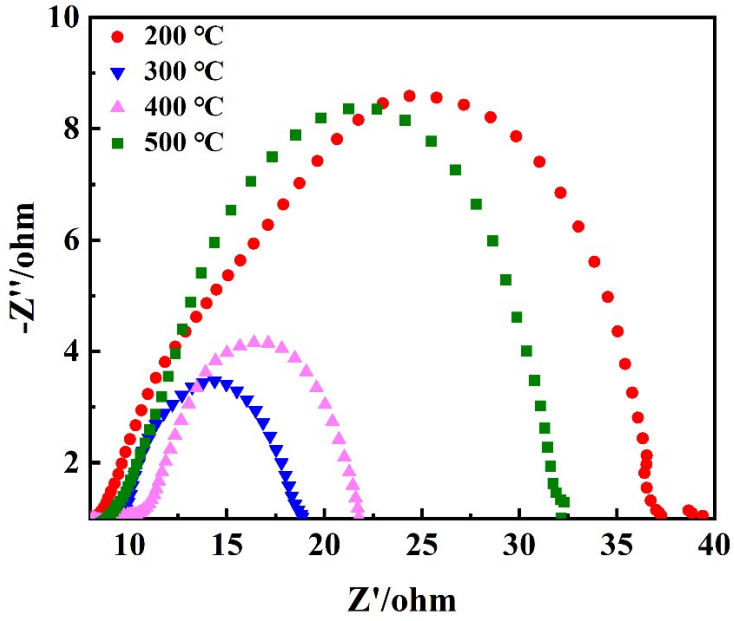

Fig. S15. EIS Nyquist plots at different annealing temperatures.

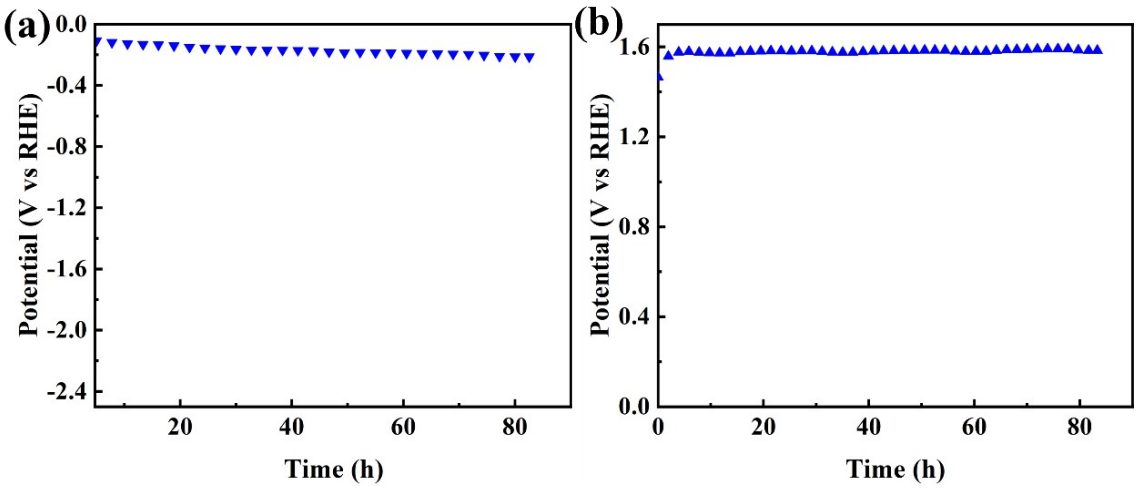

Fig. S16. (a) HER and (b) OER stability of *fcc* Ru-RuO_2/C, respectively.

Table S1. Comparation of the overpotential of the OER, HER, and OWS over *fcc* Ru-RuO_2/C with the reported noble metal electrocatalysts at 10 mA cm^{-2} under alkaline solution.

Catalyst	η_{10} (mV) HER	OER	References
***Fcc* Ru-RuO_2/C**	**30**	**283**	**This Work**
Ru_1Ni_1-NCFs	35	290	Adv. Sci. 2020, 7, 1901833.[1]
RuΔc→h/C	41	/	Adv. Mater. 2021, 33, 2105248. [2]
$RuSe_2$/CNTs-650	44	/	J. Mater. Chem. A 2022, 10, 7637. [3]
Ru-$Ni(OH)_2$	/	295	Chem. Eng. J. 2022, 429, 132478. [4]
RuOx-nc@Co_3O_4-250	/	280	Energy Storage Mater. 2020, 32, 20-29. [5]
MoOx-Ru *fcc*	20	/	ACS Nano 2022, 16,14885−14894.[6]
Ru-H_2O/CC	44	270	Applied Catalysis B: Environmental 317(2022)121729.[7]
$PtSe_2$/Pt	42	/	Angew. Chem. Int. Ed. 2021, 60, 23388. [8]
3D $RhSe_2$	81	/	Adv. Mater. 2021, 33, 2007894.[9]

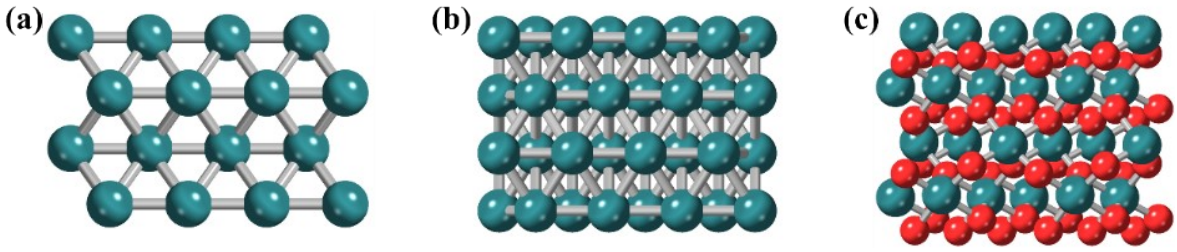

Fig. S17. The geometric structure.(a) *fcc* Ru (b) *hcp* Ru and (c) RuO_2.

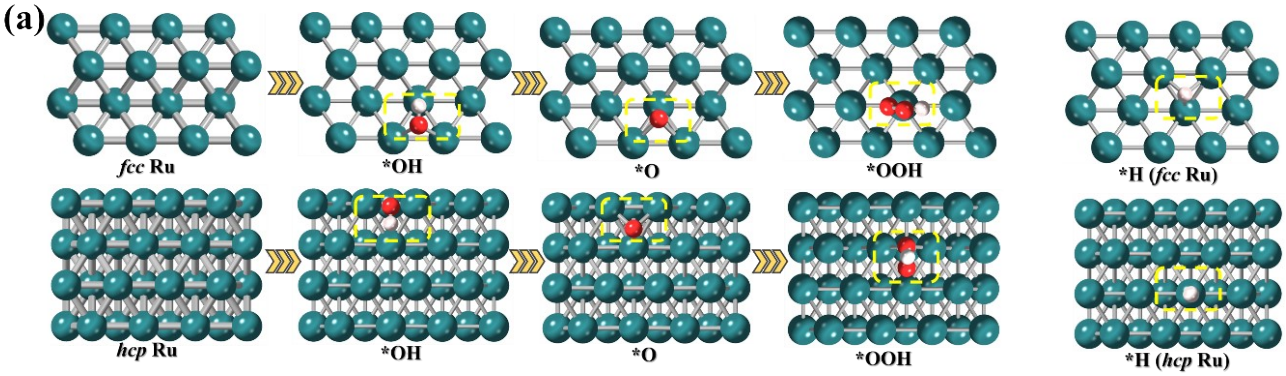

Fig. S18. The theoretical study. (**a**) Schematic illustration of the atomic structures of intermediate adsorption on *fcc* Ru and *hcp* Ru during HER and OER process.

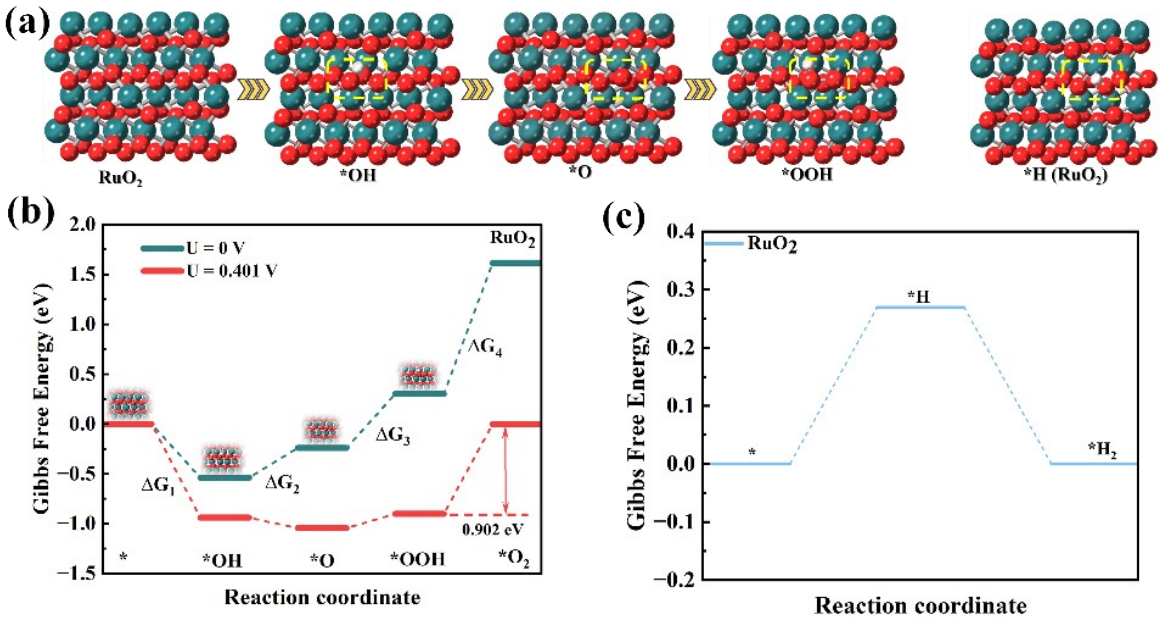

Fig. S19. The theoretical study. (**a**) Schematic illustration of the atomic structures of intermediate adsorption on RuO_2 during HER and OER process. (**b**, **c**) The calculated corresponding free-energy diagram of the HER and OER.

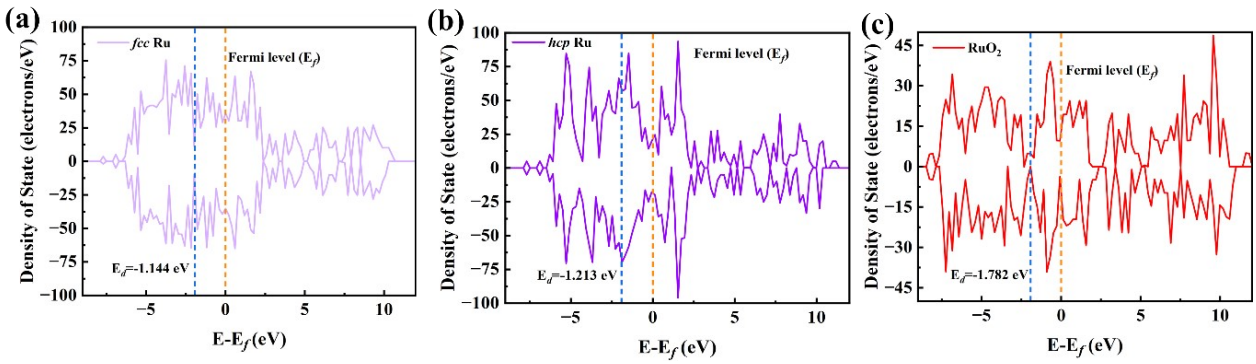

Fig. S20. The d-band centers of (**a**) *fcc* Ru. (**b**) *hcp* Ru. (**c**) RuO_2.

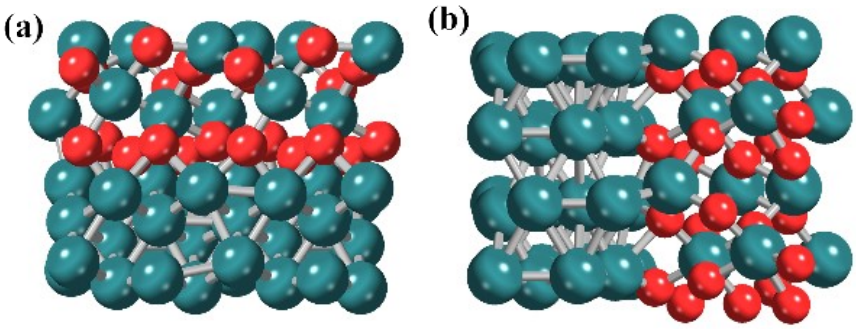

Fig. S21. The geometric structure of *fcc* Ru- RuO_2 and *hcp* Ru- RuO_2.

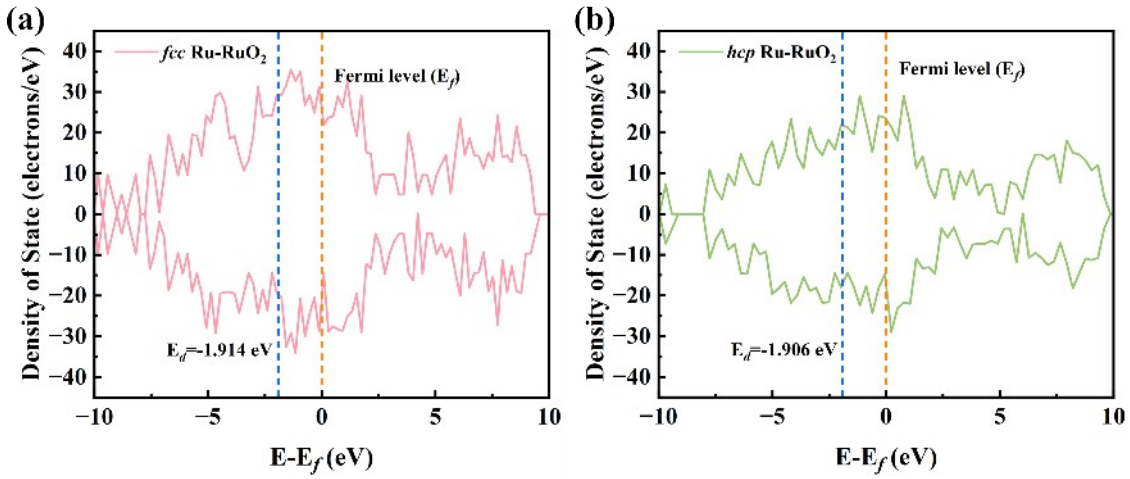

Fig. S22. Projected DOS and d band of *fcc* Ru- RuO_2 and *hcp* Ru- RuO_2.

References

[1]M. Li, H. Wang, W. Zhu, W. Li, C. Wang and X. Lu. *Adv. Sci*. **2020**, *7*, 1901833.

[2]J. Kim, H. J. Kim, B. Ruqia, M. J. Kim, Y.-J. Jang, T. H. Jo, H. Baik, H.-S. Oh, H.-S. Chung, K. Baek, S. Noh, M. Jung, K.-j. Kim, H.-K. Lim, Y.-S. Youn and S.-I. Choi. *Adv. Mater.* **2021**, *33*, 2105248.

[3]D. Chen, R. Lu, Y. Yao, D. Wu, H. Zhao, R. Yu, Z. Pu, P. Wang, J. Zhu, J. Yu, P. Ji, Z. Kou, H. Tang and S. Mu. *J. Mater. Chem. A*. **2022**, *10*, 7637.

[4]R. Guo, W. Shi, Wenzhu Liu, X. Yang, Y. Xie, T. Yang and J. Xiao. Chem. Eng. J. **2022**, *429*, 132478.

[5]Q. Lu, Y. Guo, P. Mao, K. Liao, X. Zou, J. Dai, P. Tan, R. Ran, W. Zhou, M. Ni and Z. Shao. *Energy Storage Mater.* **2020**, *32*, 20.

[6] L. Li, C. Liu, S. Liu, J. Wang, J. Han, T. S. Chan, Y. Li, Z. Hu, Q. Shao, Q. Zhang and X. Huang. *ACS Nano*. **2022**, *16*, 14885.

[7] M. You, X. Du, X. Hou, Z. Wang, Y. Zhou, H. Ji, L. Zhang, Z. Zhang, S. Yi and D. Chen. *Applied Catalysis B: Environmental*. **2022**, *317*, 121729.

[8]Z. Wang, B. Xiao, Z. Lin, Y. Xu, Y. Lin, F. Meng, Q. Zhang, L. Gu, B. Fang, S. Guo and W. Zhong. *Angew. Chem. Int. Ed*. **2021**, *60*, 23388.

[9] W. Zhong, B. Xiao, Z. Lin, Z. Wang, L. Huang, S. Shen, Q. Zhang and L. Gu. *Adv. Mater.* **2021**, *33*, 2007894.